EPTT 2024
Escola de Primavera de Transição e Turbulência

ABCM
Associação Brasileira de Engenharia e Ciências Mecânicas

EPTT-2024-0056
Boundary integral simulations based on the vortex sheet formalism applied to track droplet interfaces in Hele-Shaw cells

Rafael M. Oliveira
Pedro H. A. Anjos
Departamento de Engenharia Mecânica, Pontifícia Universidade Católica do Rio de Janeiro, Rio de Janeiro RJ 22451-900, Brazil
rmo@puc-rio.br, pamorimanjos@esp.puc-rio.br

Abstract. *We track nonlinear deformations of liquid droplets confined between the two parallel plates of a Hele-Shaw cell. The viscous droplet is surrounded by a fluid of different viscosity, and its interface is governed by surface tension. Both fluids satisfy Darcy's law, which makes flow in their bulk potential and irrotational. As a result, vorticity is concentrated at the sharp interface between them. This allows for the discretization of the interface based on an accurate boundary integral method written in terms of the vortex sheet. This quantity measures the jump of the tangential velocity component as one crosses the interface. It is related to and better suited than vorticity to track sharp interface deformations. Application of Darcy'law and the Young-Laplace pressure jump boundary condition allows to write a Birkhoff-Rott integral equation for the distribution of vortex sheet in every time step, which is discretized by the modified point vortex approximation. Time evolution of the interfacial shape is conducted by integrating in time the interface velocity written in terms of the vortex sheet. This is accomplished by writing the evolution equations in terms of the tangent angle and arclength. This change of variables is motivated by the Frenet-Serret identity that relates derivatives of the tangent angle with planar curvatures. This reduces the order of the differential equations and, alongside the small-scale decomposition, also removes stiffness. The final evolution equations have spectral accuracy, are linear, and are solved by the Adams-Bashforth algorithm. We discuss this methodology and present results for different Hele-Shaw flow configurations, including (i) Growth of viscous fingers by radial injection; (ii) Droplet deformations related to adhesion phenomena and driven by air invasion when the top plate is lifted; and (iii) Deformations of magnetic droplets subjected to crossed magnetic fields.*

Keywords: *Boundary integral method, Hele-Shaw cell, Fingering instability*

1. INTRODUCTION AND METHODOLOGY

A canonical device in the investigation of interfacial instabilities is the Hele-Shaw cell, composed of two flat, parallel plates placed close to each other. This confined system brings similarities to flows in porous media and allows us to investigate details of the physics and of the processes that generate fingering instabilities that arise in the movement between fluids. A classic example is the Saffman-Taylor instability (Saffman and Taylor (1958); Homsy (1987); McCloud and Maher (1995)), which describes the formation of viscous fingers when a fluid is displaced by a less viscous one. This system is governed by the viscosity between the fluids, the surface tension of the interface between them, and the injection rate. Here, we discuss a boundary integral technique based on the vortex sheet formalism that describes nonlinear interfacial deformations with accucary. We apply this technique and present a few numerical results of the Saffman-Taylor problem in addition to investigate important problem variations.

The physical system consists of a Hele-Shaw cell of thickness b containing immiscible Newtonian fluids. Between the fluids there is an interface with surface tension σ, cf. Fig. 1. In this nearly two-dimensional scenario, our hydrodynamic problem is described by Darcy's law

$$\mathbf{v}_j = -\frac{b^2}{12\eta_j}\nabla p_j, \tag{1}$$

and the incompressibility condition

$$\nabla \cdot \mathbf{v}_j = 0, \tag{2}$$

where $\mathbf{v}_j$ e p_j represent, respectively, the average velocity through the Hele-Shaw plates and the pressure in fluid j. The interfacial movements are determined by the governing equations (1) and (2), plus moving boundary conditions at each

(a) (b)

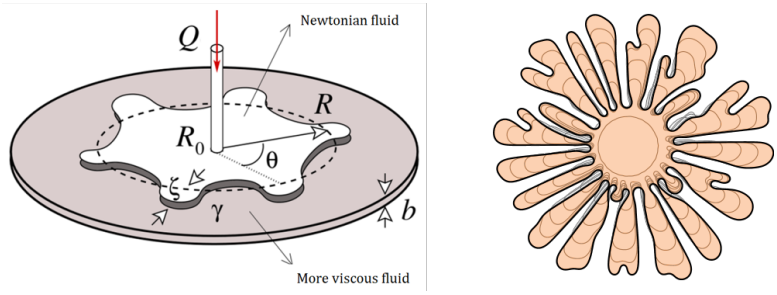

Figure 1. (a) A less viscous fluid is injected at aerial rate Q to displace a more one in a Hele-Shaw cell of gap width b leading to the growth of viscous fingering instabilities; (b) Simulation results showing a time evolution at different gray lines when the viscosity contrast between the fluid is high.

fluid-fluid interface. These are given by the Young-Laplace equation for the pressure jump and by the kinematic boundary condition that states that the normal component of velocity is continuous across the interface. These conditions are given by

$$(p_1 - p_2) = \sigma\kappa \qquad \text{and} \qquad (\mathbf{v}_1 \cdot \hat{n}) = (\mathbf{v}_2 \cdot \hat{n}). \tag{3}$$

In these equations, κ is the interfacial curvature in the plane and $\hat{n}$ is the unit normal vector at the interface. Because of Darcy's law, the velocity field in the bulk of each fluid is potential and irrotational. As a result, vorticity is concentrated at the sharp interface between them. This allows for the discretization of the interface based on an accurate boundary integral method written in terms of the vortex sheet. This quantity measures the jump of the tangential velocity component as one crosses the interface. It is related to and better suited than vorticity to track sharp interface deformations. It is given by

$$\gamma = s_\alpha(\mathbf{v}_2 - \mathbf{v}_1) \cdot \hat{s} = 2As_\alpha \mathbf{W} \cdot \hat{s} + \frac{b^2\sigma}{6(\eta_1 + \eta_2)} s_\alpha k_s \tag{4}$$

where $\kappa_s \equiv \partial\kappa/\partial s$ and

$$A = \frac{\eta_1 - \eta_2}{\eta_1 + \eta_2} \tag{5}$$

is the first dimensionless parameter of the problem, known as viscosity contrast. On the other hand, the average interface velocity $\mathbf{W} = (\mathbf{v}_1 + \mathbf{v}_2)/2$ can be represented by a boundary integral term, yielding (Tryggvason and Aref, 1983)

$$\mathbf{W}(\alpha, t) = +\frac{1}{2\pi}\mathrm{P}\int_0^{2\pi} \tilde{\gamma}(\alpha', t)\frac{\hat{\mathbf{z}} \times [\mathbf{\Gamma}(\alpha, t) - \mathbf{\Gamma}(\alpha', t)]}{|\mathbf{\Gamma}(\alpha, t) - \mathbf{\Gamma}(\alpha', t)|^2} d\alpha', \tag{6}$$

where the P denotes the principal value integral. The interface position is $\mathbf{\Gamma}(\alpha, t) = x(\alpha, t)\hat{\mathbf{x}} + y(\alpha, t)\hat{\mathbf{y}}$ with $x(\alpha, t)$ and $y(\alpha, t)$ representing the time-dependent coordinates parameterized by the azimuthal angle $\alpha = [0, 2\pi]$. Equation (4) is a Birkhoff-Rott integral equation for the distribution of vortex sheet. It is solved in every time step by the modified point vortex approximation.

Notice that the equations above are general statements and some adaptation is required for each specific physical problem. For example, the growth of viscous fingering driven by injection (Fig. 1) requires inclusion of the source term, Q. For the variable gap problem in which lifting of the top Hele-Shaw plate drives fingering formation (Fig. 2) the gap width becomes a function of time, $b = b(t)$, and mass conservation for the gap-averaged velocity field modifies to $\nabla \cdot \mathbf{u}_j = -\frac{\dot{b}(t)}{b(t)}$. Moreover, when the fluid droplet is magnetic, deformation can also be controlled by applying an external magnetic field. This requires modifying Darcy's law to include magnetic body forces and updating the pressure jump boundary condition to include a dependence on the magnetization of the material.

Common to all problems is the influence of surface tension at the interface between the internal and external fluids. This term depends on the curvature κ and introduces large a number of spatial derivatives, leading to numerical stiffness. This motivates application of the Frenet-Serret identity that relates derivatives of the tangent angle with planar curvatures, $\theta_s = \kappa$, where subscripts refer to partial differentiation, θ is the tangent angle and s denotes the arclength.

Time evolution equations of the plane interfacial curve can be obtained from $\mathbf{\Gamma}_t(\alpha, t) = x_t(\alpha, t)\hat{\mathbf{x}} + y_t(\alpha, t)\hat{\mathbf{y}} = U\hat{\mathbf{n}} + T\hat{\mathbf{s}}$, where $U = \mathbf{W} \cdot \hat{\mathbf{n}}$ and $T = \mathbf{W} \cdot \hat{\mathbf{s}}$ are the normal and tangential components of the interface velocity, respectively. Interestingly, it is possible to rewrite these equations in terms of θ_α and s_α:

$$s_{\alpha,t} = T_\alpha - U\theta_\alpha, \tag{7}$$

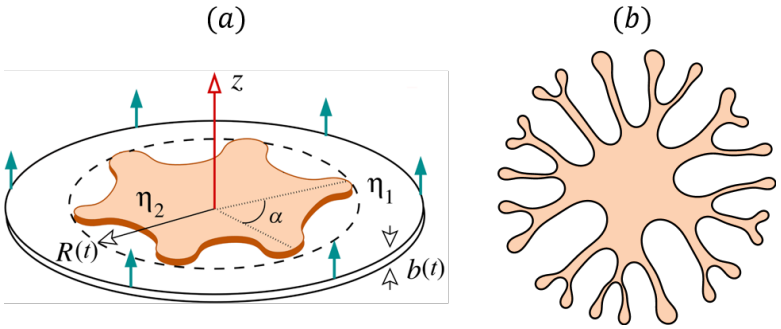

Figure 2. (a) Internal viscous droplet is stretched by lifting the top plates at an exponential rate. The Hele-Shaw gap becomes time dependent, $b = b(t)$. (b) Simulation result shows typical fingering structures when a fluid of negligible viscosity (air) surrounds the droplet.

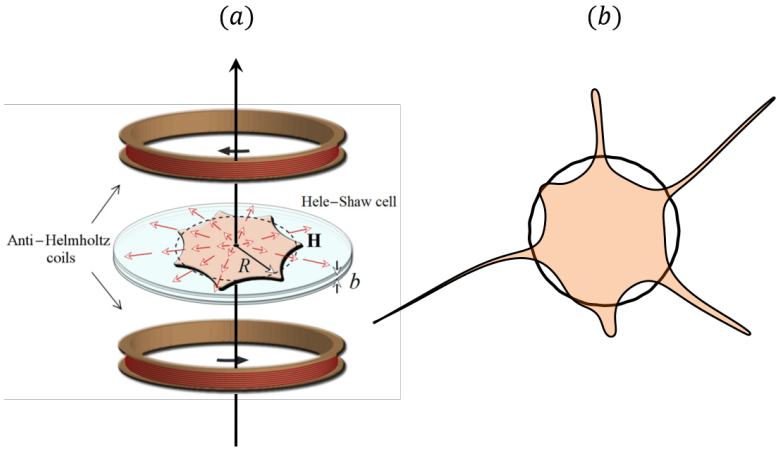

Figure 3. (a) Ferrofluid droplet subjected to the influence of two magnetic fields. The radial field is generated by two coils in the anti-Helmzoltz configuration and the azimuthal field generated by a current-carrying wire passing through the center of the domain (b) The magnetic fields tends to spread the droplet radially forming spiky fingers. In addition, the combined influence of the fields induces a rotation to the droplet as it deforms (**??**).

$$\theta_t = \frac{1}{s_\alpha}(U_\alpha + T\theta_\alpha). \tag{8}$$

However, notice that both U and T depends on the vortex sheet. So, the above set of equations are integro-differential and difficult to solve. To linearize equation (8) and reduce its stiffness, we take advantage of the small-scale decomposition described by Hou *et al.* (1994). Simplification can be achieved by introducing complex variables $z = x + iy$. This allows one to write the term which is the main source of stiffness as a Hilbert transform of spatial derivatives of θ. Then, to linearize, we take advantage of the interesting property that the Hilbert transform diagonalizes under the Fourier transform and solve this governing equation for the transformed variable. The second governing equation, Eq. (7), can be simplified by making s_α constant so that $s_\alpha = L(t)/(2\pi)$. This allows us to track the perimeter of the interface, $L(t)$, by integrating it with an Adams-Bashforth method.

2. NUMERICAL RESULTS

We present one result of three different physical problems in order to explore the accuracy of the methodology and its adaptability. These problems are controlled by at least two governing parameters: the viscosity contrast, A, and an effective surface tension B, that normalizes surface tension by an influence directly related to instability growth.

Figure 1 investigates the classical viscous fingering problem that appear when a less viscous fluid is injected to displace a more viscous one. This radial version of the Saffman-Taylor problem is considered by imposing a constant injection rate, Q, and by injecting a fluid of negligible viscosity ($A = 1$) to drive fingering formation. The B-parameter is normalized by the injection rate and defined as $B = \pi b^2\sigma/(6\eta Q R_0)$, where σ is the surface tension at the interface, η is the viscosity of the displaced fluid, Q is the areal injection rate, and R_0 is the initial droplet radius. Figure 1(b) presents a simulation result. The internal gray curves is nearly circular and depicts the initial condition. Successive gray curve indicate time evolution and the final simulated time has black contours and is painted in the interior. A detailed discussion of this problems has been published by Oliveira *et al.* (2023).

Figure 2 consider a variation of the traditional viscous fingering problem which appears when the top Hele-Shaw plate is lifted. As the plate is lifted up, the air invades the nearly circular droplet, deforming it. This variable gap problem is associated to probe-tack experiments and adhesion phenomena (Sinha *et al.* (2008); Anjos *et al.* (2022)). We are interested in conducting a detailed parametric study considering different lifting rates. In the numerical algorithm this is captured in dimensionless form by the B parameter, which now compares surface tension to the initial lifting velocity. An open question in the literature we are interested in addressing concerns the lifting force. Does late-time, large amplitude deformation of the contracting interface influence the adhesive response of the fluid sample? In this regard, the simulation result shown in Figure 2(b) is preliminary.

Finally, Figure 3 analyzes the morphology of the interface separating a ferrofluid droplet and a nonmagnetic fluid in a Hele-Shaw cell, when crossed radial and azimuthal magnetic fields are applied. An in-depth discussion regarding the morphology and dynamics of this system has been published by Oliveira *et al.* (2021). The effective surface tension parameter, B, is now normalized by the magnitude of the magnetic field, and the problem is also controlled by additional parameters, namely, the magnetic susceptibility, and the relative influence of the azimuthal and radial fields. It is noteworthy for the current numerical purposes to observe the elongated sharp finger that are accurately captured by the boundary integral simulation.

3. CONCLUSIONS

The current work summarizes the boundary integral method based on the vortex sheet formalism employed to discretize the sharp interface between fluids of different viscosities confined between the parallel plates of a Hele-Shaw cell. The interface is governed by surface tension and its curvature introduces numerical stiffness to the equations. The governing equations are given by Darcy's law and moving boundary conditions are applied at the interface. Interface deformations are tracked by the vortex sheet, a quantity that measures the discontinuity of the tangential component of velocity at the interface. We highlight that only the interface discretized. This makes the method effectively one-dimensional. It employs the small-scale decomposition to remove stiffness, has spectral accuracy and time integration is achieved by simple Adams-Bashforth algorithms. The numerical method has been applied to capture morphological details of the interface for three different Hele-Shaw configurations: (i) Growth of viscous fingers driven by radial injection; (ii) Droplet deformations driven by air injection when the top plate is lifted; and (iii) Deformations of a magnetic droplets subjected to the combined influence of the radial and azimuthal magnetic fields.

4. REFERENCES

Anjos, P.H., Rocha, F.M. and Dias, E.O., 2022. "Controlling fluid adhesion force with electric fields". Vol. 106, No. 5, p. 055109.

Homsy, G.M., 1987. "Viscous fingering in porous media". Vol. 19, pp. 271–311.

Hou, T.Y., Lowengrub, J.S. and Shelley, M.J., 1994. "Removing the stiffness from interfacial flows with surface tension". Vol. 114, No. 2, pp. 312–338.

McCloud, K.V. and Maher, J.V., 1995. "Experimental perturbations to Saffman-Taylor flow". Vol. 260, No. 3, pp. 139–185.

Oliveira, R.M., Abedi, B., Santos, L.F., Camara, P.S. and de Souza Mendes, P.R., 2023. "Similarity characteristics in the morphology of radial viscous fingers". Vol. 35, No. 042114.

Oliveira, R.M., Coutinho, I.M., Anjos, P.H.A. and Miranda, J.A., 2021. "Shape instabilities in confined ferrofluids under crossed magnetic fields". Vol. 104, No. 065113.

Saffman, P.G. and Taylor, G.I., 1958. "The penetration of a fluid into a porous medium or Hele-Shaw cell containing a more viscous liquid". Vol. 245, p. 312.

Sinha, S., Dutta, T. and Tarafdar, S., 2008. "Adhesion and fingering in the lifting Hele-Shaw cell: Role of the substrate". Vol. 25, pp. 267–275.

Tryggvason, G. and Aref, H., 1983. "Numerical experiments on Hele-Shaw flow with a sharp interface". Vol. 136, pp. 1–30.

5. RESPONSIBILITY NOTICE

The authors are the only responsible for the printed material included in this paper.